Chemical Science

ROYAL SOCIETY OF CHEMISTRY

EDGE ARTICLE

View Article Online
View Journal | View Issue

Cite this: *Chem. Sci.*, 2020, **11**, 1643

All publication charges for this article have been paid for by the Royal Society of Chemistry

Received 30th November 2019
Accepted 30th December 2019

DOI: 10.1039/c9sc06064b

rsc.li/chemical-science

Seed-mediated evolution of hierarchical metal–organic framework quaternary superstructures†

Liang Feng,[a] Kun-Yu Wang,[a] Tian-Hao Yan[a] and Hong-Cai Zhou *[ab]

The idea of hierarchy, widely observed in natural and artificial worlds, has been extensively explored in chemistry and materials science. Similar to proteins which contain primary, secondary, tertiary and quaternary structures, varying levels of hierarchy in metal–organic framework (MOF) superstructures can also be achieved. In this work, we initiate a systematic study on the morphological evolution of hierarchical superstructures with the assistance of seeded growth and explore the assembly of multiple modular MOFs into superstructures with enhanced hierarchy and diversity. By utilizing MOF-74-III spherulite superstructures as seeds, multiple quaternary architectures were obtained depending on the lengths of organic linker precursors. The resulting superstructures with superior hierarchy represent a unique porous material which contains multiple modules with diverse morphologies. To the best of our knowledge, this is the first report that utilizes tertiary superstructures as seeds in MOF synthesis, which leads to unusual and diverse behaviors during secondary growth. This synthetic approach not only provides a facile method to establish hierarchy in porous materials, but also enables the fabrication of multiscale heterostructures through secondary growth on MOF seeds.

Introduction

Complex materials with hierarchical structures have demonstrated unusual properties and behaviors, which has attracted increasing attention in recent years.[1,2] As a class of porous crystalline materials constructed from organic linkers and inorganic clusters, metal–organic frameworks (MOFs) present a promising platform to conjugate multiple modules into one integrated system.[3–6] The placement of functionalities that can complete tandem chemical processes would allow for intrinsic tunability over pore environments in hierarchical MOF systems with heterocompositions.[7–10] Therefore, MOF architectures with well-defined modules and sequences provide great opportunities in extensive fields such as drug delivery, catalysis and sensing.[11–13]

Seed-mediated growth is considered a viable pathway for fabricating sophisticated architectures.[14–16] Jiang, Zhou and coworkers reported the synthesis of phase-pure MOFs by introducing seed crystals.[17] Consequently, the formation of mixed nuclei could be hindered during the nucleation stage, leading to the growth of phase-pure MOFs. Oh and co-workers reported isotropic and anisotropic growth of a secondary MOF, depending on its lattice parameters, during the growth of core–shell MIL-68@MIL-68-Br and semitubular particles MIL-68@MOF-NDC.[18] Furthermore, Zhou and co-workers introduced the concept of retrosynthesis to engineer the compositions, ratios and distributions of hierarchical MOF-on-MOF structures.[19] The modular synthesis can further be programmed to tailor hierarchy and diversity in multivariate systems.[20] Later, Rosi and co-workers constructed multilayer core–shell MOFs using domain building blocks, which endows MOFs with enhanced diversity and functionalities.[21] Very recently, Li and co-workers unveiled two kinetic factors, nucleation and dissolution kinetics, which play important roles in fabricating hierarchical structures with unprecedented complexity.[22] However, all these examples featured a limited level of hierarchy, simply because the seed crystals are intrinsically single crystals rather than superstructures. Therefore, considering the limited hierarchical complexity of the assembled MOF superstructures, the assembly of quaternary superstructures outside seed crystallites that already exhibit a high order of hierarchy, for example, tertiary seed superstructures, remains unexplored.

In this work, we initiate a systematic study on the morphological evolution of superstructures employing seeded growth and explore the assembly of multiple modular MOFs to further enhance hierarchy and diversity of MOF superstructures. The hierarchical order of a MOF superstructure can be regarded as the number n, which is the level of scale within a specific structure (Scheme 1).[7] Similar to proteins which contain primary, secondary, tertiary and quaternary structures, the hierarchy of MOF superstructures includes primary

[a]*Department of Chemistry, Texas A&M University College Station, TX 77843, USA. E-mail: zhou@chem.tamu.edu*

[b]*Department of Materials Science and Engineering, Texas A&M University College Station, Texas 77842, USA*

† Electronic supplementary information (ESI) available. See DOI: 10.1039/c9sc06064b

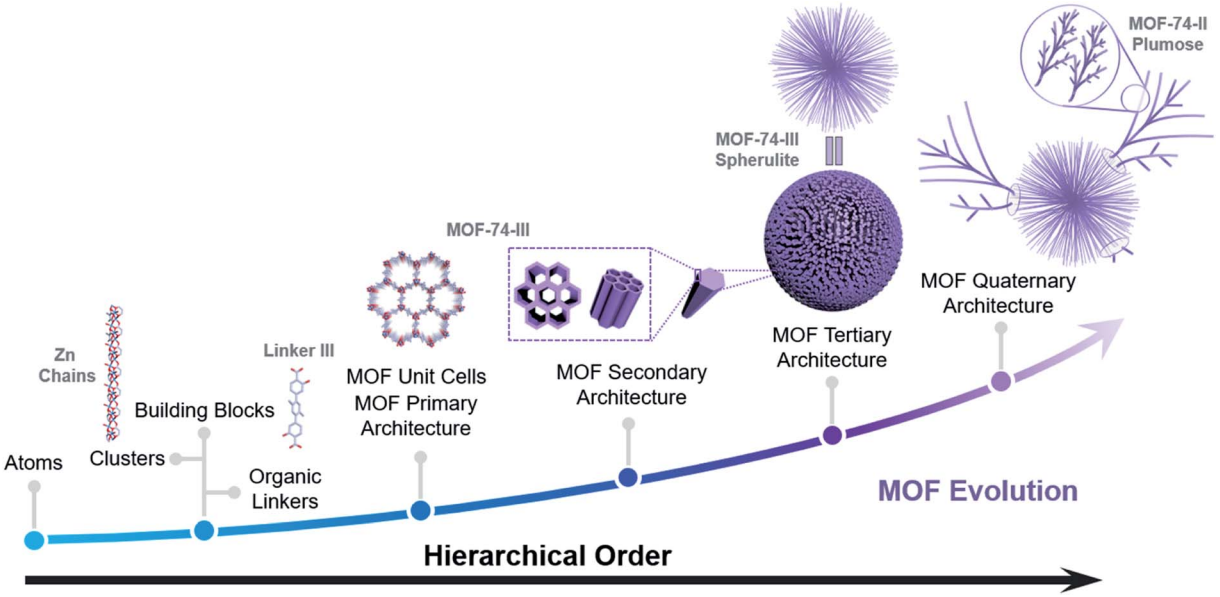

Scheme 1 Evolution illustration of hierarchical metal–organic framework (MOF) quaternary superstructures. The hierarchical order of a MOF superstructure can be regarded as the number (*n*) of levels of scale within a specific structure, which includes primary architectures (MOF unit cells) constructed from basic building blocks, secondary architectures such as MOF crystallites, tertiary architectures such as hierarchical assemblies of MOF crystallites, and more complicated quaternary architectures.

architectures (MOF unit cells) constructed from basic building blocks, secondary architectures such as MOF crystallites, tertiary architectures such as hierarchical assemblies of MOF crystallites, and more complicated quaternary architectures. By utilizing MOF-74-III spherulites as seeds, multiple quaternary architectures with superior hierarchy were obtained (Fig. 2b). The secondary evolution modes including epitaxial growth of MOF-74-III and plumose superstructures of MOF-74-II and templated evolution of MOF-74-I hollow aggregates were observed when MOF-74-III spherulites were mixed with precursors containing linkers which have either identical or different lengths. It was found that the lattice mismatch and linker acidity played vital roles in the hierarchical superstructure evolution. The level of hierarchy in these superstructures is rarely observed in coordination chemistry and is comparable to the complicated hierarchical systems found in nature such as proteins. To the best of our knowledge, this is the first report that utilizes tertiary superstructures as seeds in MOF synthesis, which leads to unusual and diverse behaviors during the secondary growth. This study indicates the design possibility of targeted complex heterostructured superstructures through seed-mediated synthesis, with precisely defined modules that can be further programmed to execute specific tasks.

Results and discussion

MOF-74 is a well-known MOF due to its great potential in storage, separation and catalysis (Fig. 2a).[23,24] Multiple research groups found that morphologies of MOF-74 could be altered by controlling the synthetic conditions, including chestnut-shell structures, superlong nanotubes, hollow tubes, ripened multi-channel tubes and helical tubular structures.[25–28] Very recently, we found that by choosing a *N*,*N*-dimethylformamide (DMF) solvent as the reaction medium, the assembly of hierarchical superstructures could be accelerated, generating MOF-74 spherulites as a final product (Fig. 1b).[29] The crystallization process could be completed within a few hours, and the

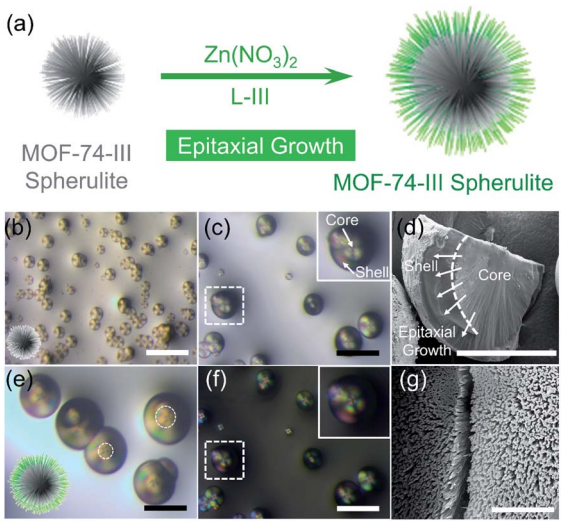

Fig. 1 Secondary epitaxial growth of MOF-74-III outside MOF-74-III spherulite seeds. (a) Illustration of epitaxial growth of MOF-74-III spherulites; (b) optical images of MOF-74-III spherulite seeds; (c and e) optical images of MOF-74-III@MOF-74-III spherulites after secondary growth; (f) optical images of MOF-74-III@MOF-74-III spherulites after secondary growth under polarized light; (d) SEM images of a cracked MOF-74-III@MOF-74-III particle showing a clear boundary between the core and the shell; (g) SEM images of spherulite surfaces. Scale bars are 100 μm in (b, c and f), 50 μm in (d and e) and 10 μm in (g).

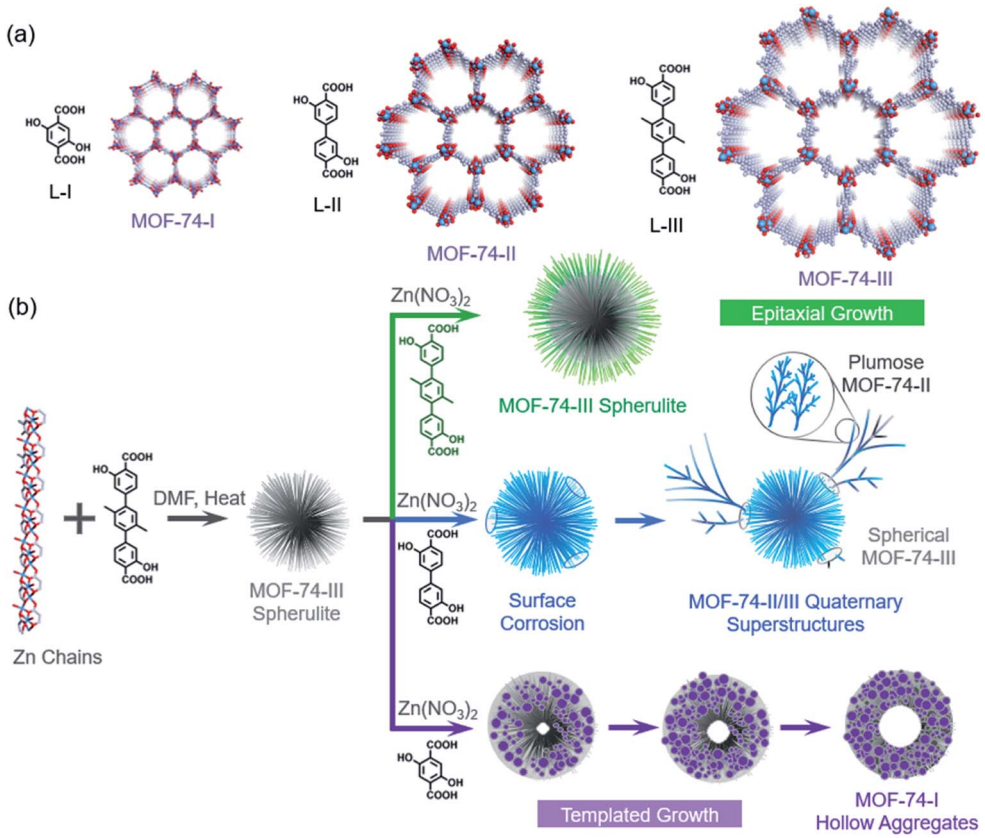

Fig. 2 Illustration of the diverse secondary growth pathways on MOF-74-III spherulites. (a) Structural illustration of MOF-74-I, II, and III and their organic building units; (b) diverse secondary growth pathways: (i) epitaxial growth of MOF-74-III spherulites was observed during secondary growth; (ii) plumose MOF-74-II crystallites tended to form on partial regions of MOF-74-III spherulites, generating a hierarchical MOF quaternary superstructure, spherical MOF-74-III/plumose MOF-74-II. (iii) MOF-74-III spherulites could be transformed into MOF-74-I hollow aggregates when replacing the original linker III of MOF-74-III with a more acidic linker I, based on a templated growth effect.

spherulite superstructures exhibited a "Maltese-cross" extinction pattern typical of spherulites under polarized light (Fig. S5†). The unique radially polycrystalline aggregates, as tertiary architecture seeds, provide an excellent platform to induce the secondary growth of quaternary spherulite superstructures.

The seeded growth of MOF-74-III spherulite superstructures was first investigated (Fig. 1). The MOF-74-III spherulites were treated with a mixture of $Zn(NO_3)_2$ and L-III DMF solution for 24 h at 100 °C. As a result, core–shell MOF-74-III@MOF-74-III was obtained (Fig. 1a). The introduction of MOF-74-III with matched crystal lattices into the precursor solution of MOF-74-III enabled heterogeneous nucleation of MOF-74-III, producing larger spherulites with a thick layer outside the original spherulites, as indicated by optical images (Fig. 1c and e). Powder X-ray diffraction (PXRD) patterns demonstrated the phase purity of the seeded growth product MOF-74-III (Fig. S6†). Optical microscopy indicates that the sizes of spherical particles changed from around 25 μm to 50 μm after epitaxial growth (Fig. 1b and c). Meanwhile, the core MOF-74-III spherulites exhibited a clear "Maltese-cross" extinction pattern while the pattern was absent in the newly formed shell layer under polarized light (Fig. 1c and f).

The morphology of resulting spherulites can be further visualized by field-emission scanning electron microscopy (FESEM, Fig. 1d and g). A clear boundary between core and shell MOF-74-III was found in a cracked spherulite particle, which further supports the epitaxial growth mechanism. It should be noted that the heterogeneous growth of MOF-74-III spherulites requires a much lower driving force by bypassing the nucleation stage than the homogeneous growth. The precursor concentration of MOF-74-III became more diluted as the seeded heterogeneous growth of MOF-74-III spherulites continued, which also impeded the homogeneous growth process.

Interestingly, when mixed with the precursors of MOF-74-II, the secondary growth of MOF-74-III seeds exhibited a totally different behavior (Fig. 3). The mixture of MOF-74-III spherulites, $Zn(NO_3)_2$ and L-II DMF solution was treated at 100 °C for 24 h. It was found that without the addition of seeds, the growth of MOF-74-II continued uniformly in all directions in homogeneous solutions, leading to the formation of MOF-74-II spherulitic aggregates due to the radial growth habit (Fig. S7†). Yet, with MOF-74-III spherulites present, plumose MOF-74-II crystallites tended to form (Fig. 3a). To better visualize the morphologies of the superstructure, we doped a small amount of a dye ligand, metal phthalocyanine $Co[Pc(COOH)_4]$, during

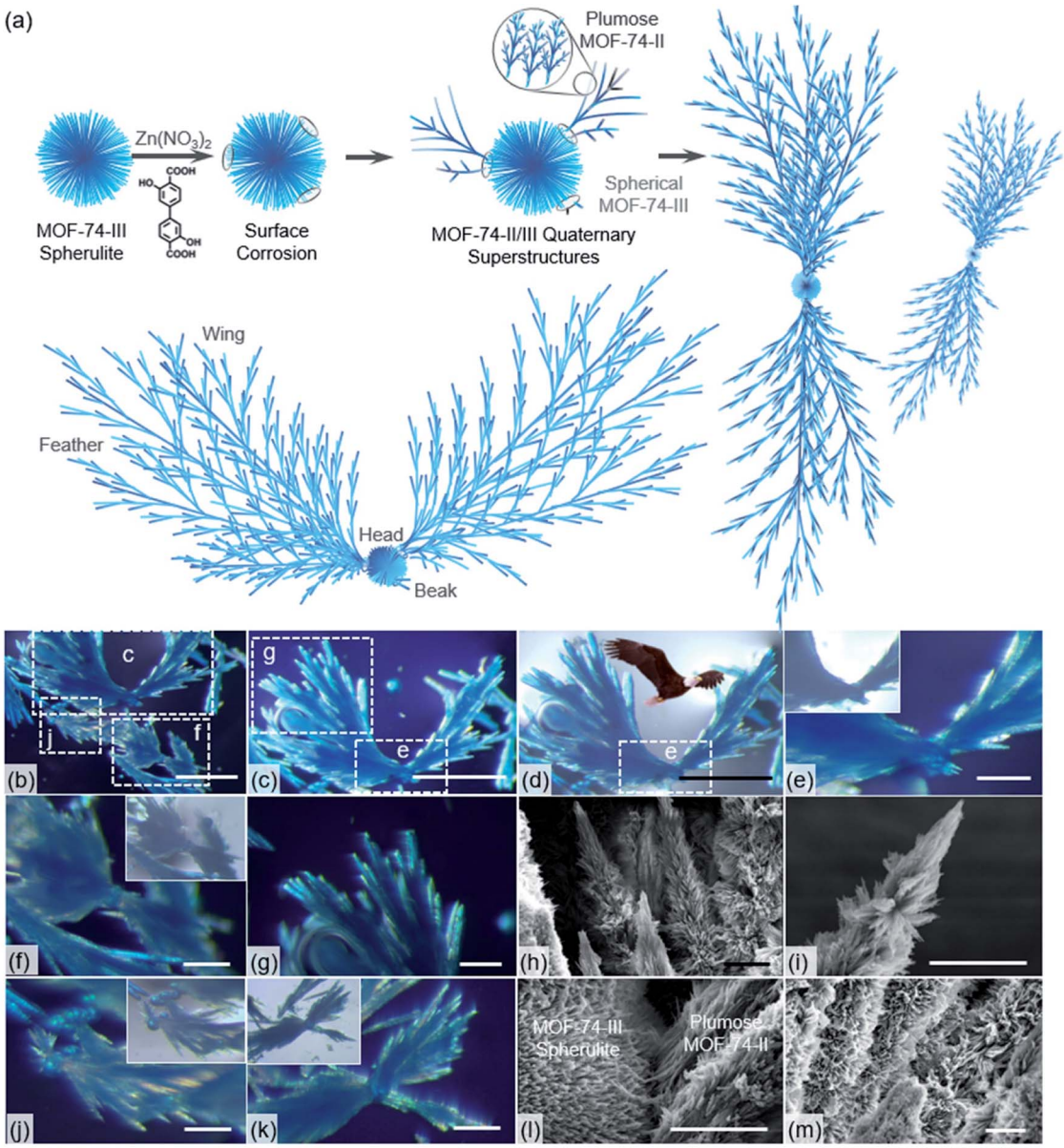

Fig. 3 Evolution of spherical MOF-74-III/plumose MOF-74-II quaternary superstructures. (a) Schematic illustration of the stepwise evolution from MOF-74-III spherulites to spherical MOF-74-III/plumose MOF-74-II quaternary superstructures. (b–g, j and k) Optical images of MOF-74-III/plumose MOF-74-II crystals, showing fractal structures; the blue color of the crystals is visualized using the doped dye, metal phthalocyanine ligand. (h, i and m) SEM images of plumose MOF-74-II fractal structures on the quaternary superstructures; (l) SEM images showing the junction interface between spherical MOF-74-III(left)/plumose MOF-74-II(right). Scale bars are 500 μm in (b–d), 100 μm in (e–g, j and k) and 10 μm in (h, i, l and m).

the evolution. The small amount of deep-blue dye molecules could decorate the superstructures without interrupting the secondary growth of MOF-74-II (Fig. 3b). We found that after the solvothermal reaction, MOF quaternary superstructures with an eagle-like morphology were formed, as indicated in Fig. 3b–e. Plumose MOF-74-II with fractal structures, similar to a wing full of feathers, was observed to grow on a MOF-74-III spherulite seed, which could be viewed as a head of the eagle. Additionally, two MOF-74-II needle crystallites, as beaks, were attached on the spherulite, generating an asymmetrically functionalized spherulite superstructure (Fig. 3e). Similar superstructures with plumose MOF-74-II growing on local regions of MOF-74-III spherulites were also observed as indicated in optical images (Fig. 3f, g, j and k). In this case, this quaternary hetero-superstructure contains two sets of tertiary superstructures: one MOF-74-III spherulite superstructure and multiple MOF-74-II plumose superstructures. These tertiary superstructures can function as building blocks that are assembled into a more complicated quaternary superstructure through interface growth. PXRD patterns indicated the presence of two phases including MOF-74-III and MOF-74-II (Fig. S6†). Additionally, the well-maintained "Maltese-cross" extinction pattern of MOF-74-

III under polarized light indicates the high chemical stability of MOF-74-III under the synthetic conditions (Figure 3e, j and k).

The morphology of spherical MOF-74-III/plumose MOF-74-II superstructures was further studied by SEM. As indicated in Fig. 3h, i and m, plumose MOF-74-II fractal structures can be well distinguished. MOF-74-II dendrites evolved with a multi-branching tree-like form, typical for a natural fractal pattern such as snowflake formation. The formation of these superstructures is quite rare in MOF chemistry. Notably, the formation of dendrites or plumose aggregates can be viewed as a result of incomplete radiation of spherulites.

When mixed with the precursors of MOF-74-II, plumose MOF-74-II crystallites tended to form on partial regions of MOF-74-III spherulites. We propose that the formation of this unusual superstructure might originate from the lattice mismatch between MOF-74-II and MOF-74-III. Under the solvothermal conditions, partial regions of MOF-III spherulite surfaces would undergo dissolution and recrystallization, generating defects which can be further utilized for nucleation and growth of MOF-74-II dendrites (Fig. 3a). This defective intermediate introduced asymmetry that led to regioselective epitaxial growth of MOF-74-II. Due to the confined environment and rapid growth rates, the growth direction of plumose MOF-74-II was limited to be radial. The junction interface between spherical MOF-74-III and plumose MOF-74-II, captured in SEM images, suggested the intergrowth of two lattice-mismatched MOFs (Fig. 3l).

We further explored the seeded growth behavior of MOF-74-I based on MOF-74-III spherulite seeds (Fig. 4). MOF-74-III spherulite seeds were used as a scaffold for the fabrication of hierarchical structures. When exposed to the precursor solution of MOF-74-I, the MOF-74-III spherulites gradually degraded and transformed into a new spherical structure (Fig. 4c and d). After the solvothermal reaction, the MOF-74-III spherulite structures and the corresponding Maltese-cross pattern disappeared, according to the optical images, although the spherical shape of the resulting MOF-74-I product was maintained. The morphology of MOF-74-I hollow aggregates was also imaged by SEM (Fig. 4e–h). It was found that a high density of MOF-74-I nanoneedles aggregated into a hollow sphere superstructure. PXRD patterns of the products indicated the phase purity of MOF-74-I and the complete decomposition of the original MOF-74-III spherulites (Fig. S6†).

It is well-known that there is significant difference in the chemical stability of MOFs constructed from linkers with varying lengths. Typically, isoreticular MOFs with longer organic linkers exhibit relatively poorer stability, because these MOFs usually have larger cavities, which make the labile coordination bonds more exposed to coordinating molecules and also decrease their mechanical stability. The transformation mechanism involves the gradual dissolution of MOF-74-III spherulite templates and the formation of MOF-74-I nanoneedle aggregates (Fig. 4a). Due to the contracted volume of MOF-74 caused by the linker replacement of L-III by L-I, a hollow sphere was observed to form inside the aggregated superstructures (Fig. 4b). The mechanism here is similar to the templated effects we observed previously,[25] where a labile phase

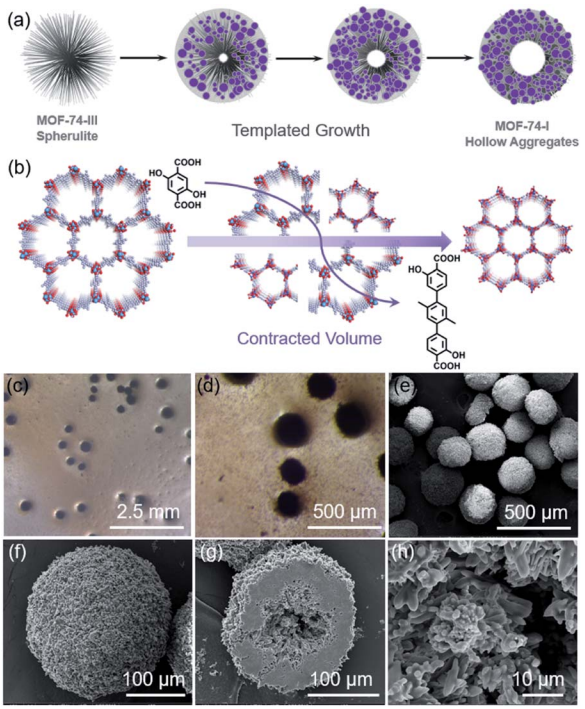

Fig. 4 Templated evolution of MOF-74-I hollow aggregates. (a) Illustration of stepwise transformation from MOF-74-III spherulites to MOF-74-I hollow sphere aggregates; (b) linker replacement of L-III by L-I leads to contracted volume of MOF-74; (c and d) optical images and (e and f) SEM images of MOF-74-I hollow sphere aggregates; (g and h) SEM images indicating the hollow structure and the aggregation of MOF-74-I needle crystallites.

PCN-74 can act as the template to induce the evolution of hollow MOF-74 tubes.

Summary and outlook

Overall, our work here explored hierarchical evolution of MOF-74 spherulite superstructures through a seed-mediated growth approach. By utilizing MOF-74-III spherulite superstructures as seeds, multiple quaternary architectures with superior hierarchy were obtained. Depending on the lengths of organic linkers, the growth of secondary MOFs on the spherulite seeds can be variable. Epitaxial growth of MOF-74-III and plumose superstructures of MOF-74-II and templated evolution of MOF-74-I hollow aggregates were observed when MOF-74-III spherulites were mixed with the precursors of secondary MOFs, respectively. The resulting superstructures represent a unique porous material which contains multiple modules with diverse morphologies and enhanced hierarchy. This study not only enables us to design the synthetic conditions of targeted MOF quaternary superstructures through seed-mediated synthesis, but also shows the possibility of controlled evolution of complex heterostructures with precisely defined modules. The formation of these superstructures with a high level of hierarchy shall allow for the hierarchical immobilization and arrangement of various catalytic species, creating new reactors for complicated and cooperative catalytic processes.

Conflicts of interest

There are no conflicts to declare.

Acknowledgements

This work was supported as part of the Center for Gas Separations, an Energy Frontier Research Center funded by the U.S. Department of Energy, Office of Science, Basic Energy Sciences under Award Number DE-SC0001015, the Robert A. Welch Foundation through a Welch Endowed Chair to H.-C. Z. (A-0030) and the Qatar National Research Fund under Award Number NPRP9-377-1-080.

References

1 F. J. Martin-Martinez, K. Jin, D. L. Barreiro and M. J. Buehler, *ACS Nano*, 2018, **12**, 7425–7433.
2 P. Fratzl and R. Weinkamer, *Prog. Mater. Sci.*, 2007, **52**, 1263–1334.
3 H. Li, M. Eddaoudi, M. O'Keeffe and O. M. Yaghi, *Nature*, 1999, **402**, 276–279.
4 H. C. Zhou and S. Kitagawa, *Chem. Soc. Rev.*, 2014, **43**, 5415–5418.
5 A. Kirchon, L. Feng, H. F. Drake, E. A. Joseph and H. C. Zhou, *Chem. Soc. Rev.*, 2018, **47**, 8611–8638.
6 J. Lee, O. K. Farha, J. Roberts, K. A. Scheidt, S. T. Nguyen and J. T. Hupp, *Chem. Soc. Rev.*, 2009, **38**, 1450–1459.
7 Y. Luo, M. Ahmad, A. Schug and M. Tsotsalas, *Adv. Mater.*, 2019, 1901744.
8 L. Feng, K.-Y. Wang, G. S. Day and H.-C. Zhou, *Chem. Soc. Rev.*, 2019, **48**, 4823–4853.
9 H. X. Deng, C. J. Doonan, H. Furukawa, R. B. Ferreira, J. Towne, C. B. Knobler, B. Wang and O. M. Yaghi, *Science*, 2010, **327**, 846–850.
10 M. Eddaoudi, J. Kim, N. Rosi, D. Vodak, J. Wachter, M. O'Keeffe and O. M. Yaghi, *Science*, 2002, **295**, 469–472.
11 A. Carne-Sanchez, I. Imaz, M. Cano-Sarabia and D. Maspoch, *Nat. Chem.*, 2013, **5**, 203–211.
12 H. J. Lee, J. We, J. O. Kim, D. Kim, W. Cha, E. Lee, J. Sohn and M. Oh, *Angew. Chem., Int. Ed.*, 2015, **54**, 10564–10568.
13 J.-S. Jang, W.-T. Koo, D.-H. Kim and I.-D. Kim, *ACS Cent. Sci.*, 2018, **4**, 929–937.
14 Y. Xia, K. D. Gilroy, H. C. Peng and X. Xia, *Angew. Chem., Int. Ed.*, 2017, **56**, 60–95.
15 A. Cacciuto, S. Auer and D. Frenkel, *Nature*, 2004, **428**, 404.
16 K. Itabashi, Y. Kamimura, K. Iyoki, A. Shimojima and T. Okubo, *J. Am. Chem. Soc.*, 2012, **134**, 11542–11549.
17 H.-Q. Xu, K. Wang, M. Ding, D. Feng, H.-L. Jiang and H.-C. Zhou, *J. Am. Chem. Soc.*, 2016, **138**, 5316–5320.
18 S. Choi, T. Kim, H. Ji, H. J. Lee and M. Oh, *J. Am. Chem. Soc.*, 2016, **138**, 14434–14440.
19 L. Feng, S. Yuan, J. L. Li, K. Y. Wang, G. S. Day, P. Zhang, Y. Wang and H. C. Zhou, *ACS Cent. Sci.*, 2018, **4**, 1719–1726.
20 L. Feng, X.-l. Lv, T.-H. Yan and H.-C. Zhou, *J. Am. Chem. Soc.*, 2019, **141**, 10342–10349.
21 T.-Y. Luo, C. Liu, X. Y. Gan, P. F. Muldoon, N. A. Diemler, J. E. Millstone and N. L. Rosi, *J. Am. Chem. Soc.*, 2019, **141**, 2161–2168.
22 F. Wang, S. He, H. Wang, S. Zhang, C. Wu, H. Huang, Y. Pang, C.-K. F. Tsung and T. Li, *Chem. Sci.*, 2019, **10**, 7755–7761.
23 H. Deng, S. Grunder, K. E. Cordova, C. Valente, H. Furukawa, M. Hmadeh, F. Gándara, A. C. Whalley, Z. Liu, S. Asahina, H. Kazumori, M. O'Keeffe, O. Terasaki, J. F. Stoddart and O. M. Yaghi, *Science*, 2012, **336**, 1018–1023.
24 E. D. Bloch, W. L. Queen, R. Krishna, J. M. Zadrozny, C. M. Brown and J. R. Long, *Science*, 2012, **335**, 1606–1610.
25 L. Feng, J.-L. Li, G. S. Day, X.-L. Lv and H.-C. Zhou, *Chem*, 2019, **5**, 1265–1274.
26 L. L. Zou, C. C. Hou, Z. Liu, H. Pang and Q. Xu, *J. Am. Chem. Soc.*, 2018, **140**, 15393–15401.
27 Y. F. Yue, Z. A. Qiao, P. F. Fulvio, A. J. Binder, C. C. Tian, J. H. Chen, K. M. Nelson, X. Zhu and S. Dai, *J. Am. Chem. Soc.*, 2013, **135**, 9572–9575.
28 L. Zou, M. Kitta, J. Hong, K. Suenaga, N. Tsumori, Z. Liu and Q. Xu, *Adv. Mater.*, 2019, e1900440, DOI: 10.1002/adma.201900440.
29 L. Feng, K.-Y. Wang, T.-H. Yan and H.-C. Zhou, *Chem*, 2019, DOI: 10.1016/j.chempr.2019.12.001.